Corrected 18 April 2024. See full text.

NEURODEGENERATION

CD4$^+$ T cells contribute to neurodegeneration in Lewy body dementia

David Gate[1,2,3]*, Emma Tapp[2,3], Olivia Leventhal[2,3]†, Marian Shahid[2], Tim J. Nonninger[2,3], Andrew C. Yang[4,5], Katharina Strempfl[6,7,8], Michael S. Unger[6,7], Tobias Fehlmann[9], Hamilton Oh[2,3], Divya Channappa[2], Victor W. Henderson[2], Andreas Keller[2,9], Ludwig Aigner[6,7], Douglas R. Galasko[10], Mark M. Davis[11,12], Kathleen L. Poston[2], Tony Wyss-Coray[2,3,5]*

Recent studies indicate that the adaptive immune system plays a role in Lewy body dementia (LBD). However, the mechanism regulating T cell brain homing in LBD is unknown. Here, we observed T cells adjacent to Lewy bodies and dopaminergic neurons in postmortem LBD brains. Single-cell RNA sequencing of cerebrospinal fluid (CSF) identified up-regulated expression of *C-X-C motif chemokine receptor 4* (*CXCR4*) in CD4$^+$ T cells in LBD. CSF protein levels of the CXCR4 ligand, C-X-C motif chemokine ligand 12 (CXCL12), were associated with neuroaxonal damage in LBD. Furthermore, we observed clonal expansion and up-regulated *interleukin 17A* expression by CD4$^+$ T cells stimulated with a phosphorylated α-synuclein epitope. Thus, CXCR4-CXCL12 signaling may represent a mechanistic target for inhibiting pathological interleukin-17–producing T cell trafficking in LBD.

Lewy body dementia (LBD) encompasses two disorders characterized by abnormal deposits of α-synuclein in the brain: dementia with Lewy bodies (DLB) and Parkinson's disease dementia (PDD). PDD is defined by changes in memory and behavior and afflicts patients in late-stage Parkinson's disease (PD) (*1*). The symptoms and cognitive profiles of DLB and PDD are highly similar (*2*). Several lines of evidence suggest involvement of the adaptive immune system in DLB (*3*) and PDD (*4*–*6*). Immune alterations have been reported in the peripheral blood of PD patients, including changes to lymphocyte activation (*7*–*9*). The involvement of CD4$^+$ T cells in PD is supported by studies in mouse models (*10*–*13*) and in vitro culture systems (*6*). Moreover, recent studies have found that a defined set of peptides derived from α-synuclein act as antigenic epitopes and promote T cell responses in nondemented PD patients ex vivo (*4*, *5*, *14*). However, demonstration of a role for T cells in the neurodegenerative process of LBD in vivo is lacking. Furthermore, the mechanism regulating T cell brain homing in LBD remains unknown.

[1]Department of Neurology, Northwestern University, Chicago, IL, USA. [2]Department of Neurology and Neurological Sciences, Stanford University School of Medicine, Stanford, CA, USA. [3]Wu Tsai Neurosciences Institute, Stanford University, Stanford, CA, USA. [4]Department of Bioengineering, Stanford University, Stanford, CA, USA. [5]Chemistry, Engineering, and Medicine for Human Health (ChEM-H), Stanford University, Stanford, CA, USA. [6]Institute of Molecular Regenerative Medicine, Paracelsus Medical University, Salzburg, Austria. [7]Spinal Cord Injury and Tissue Regeneration Center Salzburg, Paracelsus Medical University, Salzburg, Austria. [8]QPS Austria GmbH, Parkring 12, 8074 Grambach, Austria. [9]Chair for Clinical Bioinformatics, Saarland University, Saarbrucken, Germany. [10]Department of Neurosciences, University of California, San Diego, La Jolla, CA, USA. [11]Department of Microbiology and Immunology, School of Medicine, Stanford University, Stanford, CA, USA. [12]Howard Hughes Medical Institute, Stanford University School of Medicine, Stanford, CA, USA.
*Corresponding author. Email: dgate@northwestern.edu (D.G.); twc@stanford.edu (T.W.-C.)
†Present address: University of California San Francisco School of Medicine, University of California San Francisco, San Francisco, CA, USA.

Results

Neurodegeneration in LBD study subjects

To assess adaptive immunity in LBD, we integrated analyses of multiple cohorts consisting of healthy aged controls (n = 162) and patients with clinical DLB and PD (collectively referred to as PD-DLB; n = 148) (fig. S1A, table S1, and data S1). Montreal Cognitive Assessment scores indicated reduced cognition in PD-DLB subjects ($P = 8.6 \times 10^{-5}$; fig. S1B). Furthermore, proteomic analysis of cerebrospinal fluid (CSF) indicated increased levels of neurofilament light chain (NEFL; P = 0.0031; fig. S1C). NEFL reflects neuronal damage in a variety of neurological disorders (*12*–*14*). Because PD has a long prodromal phase before dementia onset, we stratified patients into PD-not cognitively impaired (PD-NCI) or PDD (those with cognitive impairments and dementia) groups. Compared to healthy subjects, patients diagnosed as PDD ($P = 6.33 \times 10^{-13}$) and DLB ($P = 4.02 \times 10^{-13}$) presented with lower cognitive scores than PD-NCI patients (P = 0.83; fig. S1D). These data suggest increased neurodegeneration in our PDD and DLB subjects.

T cells home to the LBD brain and reside in close proximity to α-synuclein deposits

We next examined postmortem substantia nigra to localize and quantify T cells in LBD. Immunohistochemical analysis showed CD3$^+$ T cells in close proximity to neuronal processes labeled by the dopamine enzyme tyrosine hydroxylase (TH) in the substantia nigra of PDD and DLB brains (Fig. 1A and fig. S2A). Quantification of control (non-neurologic disease) and LBD substantia nigra indicated higher numbers of CD3$^+$ T cells in LBD (Welch's t test, P = 0.006; Fig. 1B). We then probed LBD brains for α-synuclein to determine whether T cells localize to these protein deposits. Indeed, we found CD3$^+$ T cells adjacent to α-synuclein deposits in LBD brains (fig. S2, B and C). Quantification of these cells revealed a higher percentage of CD3$^+$ T cells localized to α-synuclein deposits in LBD substantia nigra (Welch's t test, P = 0.002; Fig. 1C). We also detected CD3$^+$ T cells adjacent to Lewy neurites surrounding TH$^+$ neurons in PDD (Fig. 1D and fig. S3, A and B) and DLB substantia nigra (fig. S3C). CD3$^+$ T cells were also found near α-synuclein$^+$ Lewy bodies adjacent to vesicular glutamate transporter 1 (vGLUT1)$^+$ glutamatergic neurons in the hippocampal CA2 region (fig. S3D). Notably, CD3$^+$ T cells were also bound to Iba1$^+$ innate immune cells, which extended processes toward phosphorylated α-synuclein$^+$ Lewy bodies in PDD (Fig. 1E) and DLB (fig. S3, E and F). In mice expressing human α-synuclein (Thy1-αSyn), CD3$^+$ T cells were found adjacent to α-synuclein deposits in the midbrain (fig. S4). Thus, T cells home to the LBD brain and reside in close proximity to α-synuclein deposits.

CXCR4 is up-regulated in CD4$^+$ T cells in LBD CSF

To uncover potential mechanisms of brain entry in LBD, we performed single-cell RNA sequencing (scRNAseq) (*15*, *16*) of CSF cells isolated from age- and sex-matched healthy (n = 11) and PD-DLB (n = 11) subjects (fig. S5A). Multidimensional reduction of scRNAseq data by t-distributed stochastic neighbor embedding (tSNE) revealed clusters of immune cells (Fig. 2A). Clusters expressed marker genes corresponding to each immune cell subtype (Fig. 2B) and were not specific to group or sex (fig. S5B). Cell-type–specific differential expression of PD-DLB versus healthy CSF cell clusters revealed CD4$^+$ T cells as the most transcriptionally altered immune cell subtype (Fig. 2C and data S2). Highly differentially expressed PD-DLB CD4$^+$ T cell genes included *Janus kinase 1* (*JAK1*), a kinase essential for cytokine signaling, and the T cell activation gene *cluster of differentiation 69* (*CD69*) (Fig. 2D). The chemokine receptor gene *C-X-C motif chemokine receptor 4* (*CXCR4*) was also highly up-regulated in PD-DLB CD4$^+$ T cells (Fig. 2D). Moreover, *CXCR4* and *CD69* were highly expressed by the majority of CD4$^+$ T cells (fig. S5C). Quantification of individual subjects' CD4$^+$ T cell *CXCR4* and *CD69* expression revealed higher levels in PD-DLB versus healthy CSF (Welch's t test, P = 0.03 and P = 0.025, respectively; fig. S5D). Analysis of pathways containing *CXCR4* indicated altered metabolic and catalytic activity and response to cytokine stimulus in CD4$^+$ T cells in PD-DLB (fig. S5E). Thus, enhanced CD4$^+$ T cell cytokine signaling and activation can be observed in PD-DLB CSF.

The increase in activation of CSF CD4$^+$ T cells in PD-DLB prompted us to determine whether

Corrected 18 April 2024. See full text.

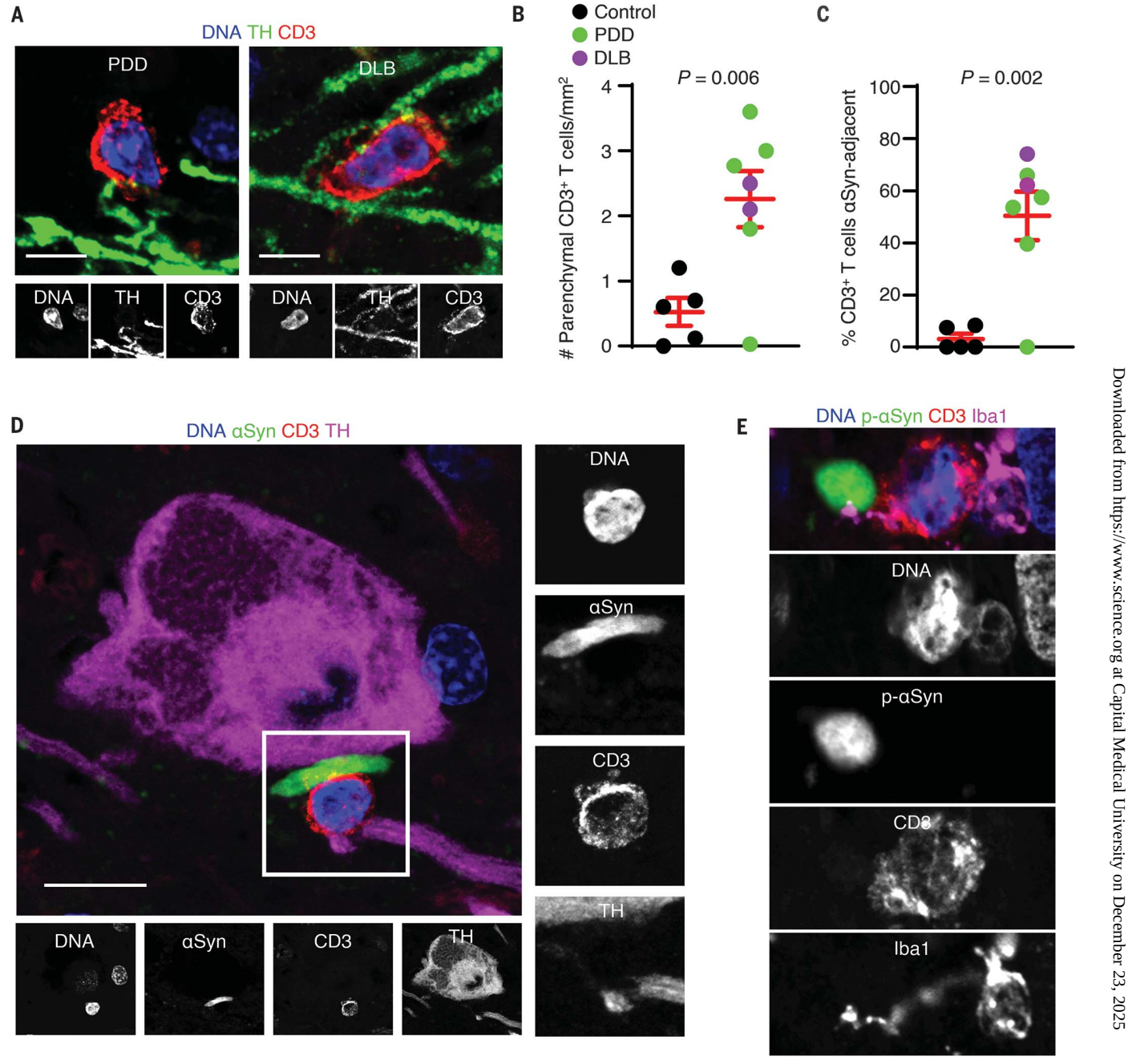

Fig. 1. T cells localize to dopaminergic neurons and α-synuclein deposits in the LBD brain. (**A**) Confocal images of parenchymal CD3$^+$ T cells adjacent to TH$^+$ neuronal processes in PDD and DLB substantia nigra. Scale bars, 10 μm. CD3$^+$ T cells were detected in six out of seven LBD brains analyzed. (**B**) Quantification of parenchymal CD3$^+$ T cells reveals higher numbers of T cells in LBD versus healthy substantia nigra. Data are mean ± SEM. (**C**) Quantification of percent parenchymal CD3$^+$ T cells adjacent to α-synuclein deposits in LBD brains. Cells determined to be adjacent to α-synuclein deposits were within 5-μm distance. Data are mean ± SEM. (**D**) Confocal image of PDD substantia nigra showing a CD3$^+$ T cell in close proximity to an α-synuclein$^+$ Lewy neurite. Scale bar, 10 μm. Similar results were observed in six out of seven LBD brains. (**E**) An Iba1$^+$ innate immune cell in the PDD substantia nigra. The Iba1$^+$ process appears to contact the CD3$^+$ T cell and α-synuclein$^+$ Lewy body in PDD. Scale bar, 5 μm. Similar results were observed in six out of seven LBD brains.

clonally expanded (i.e., antigen-specific) cells were distinct in PD-DLB. To assess clonal expansion, we performed single-cell T cell receptor sequencing (scTCRseq) on the same CSF cells as above (Fig. 2E). Comparing RNA transcriptomes of clonal CD4$^+$ T cells from healthy and PD-DLB CSF by differential expression again showed increased expression of *CD69* and *CXCR4* in PD-DLB (Fig. 2, F and G, and data S3). Clonal T cells were not specific to disease group or sex (fig. S6A). Pathway analysis of differentially expressed clonal CD4$^+$ PD-DLB T cell genes revealed regulation of cytokine-mediated signaling and intracellular signal transduction as the most altered pathways containing *CXCR4* (fig. S6B). We also detected higher expression of *killer cell lectin-like receptor subfamily B, member 1* (*KLRB1*),

Corrected 18 April 2024. See full text.

a marker of proinflammatory interleukin-17 (IL-17)–producing [T helper 17 (T_H17)] memory $CD4^+$ T cells (*17*, *18*) (Fig. 2F and data S3). We also localized $CD3^+KLRB1^+$ T cells to phosphorylated α-synuclein deposits in the parenchyma of PDD brains (fig. S6C). Thus, LBD may involve enhanced activation of proinflammatory $CD4^+$ T_H17 cells.

The CXCR4 ligand CXCL12 is associated with neurodegeneration in LBD

To determine if T cells express CXCR4 in the brain, we performed immunohistochemistry

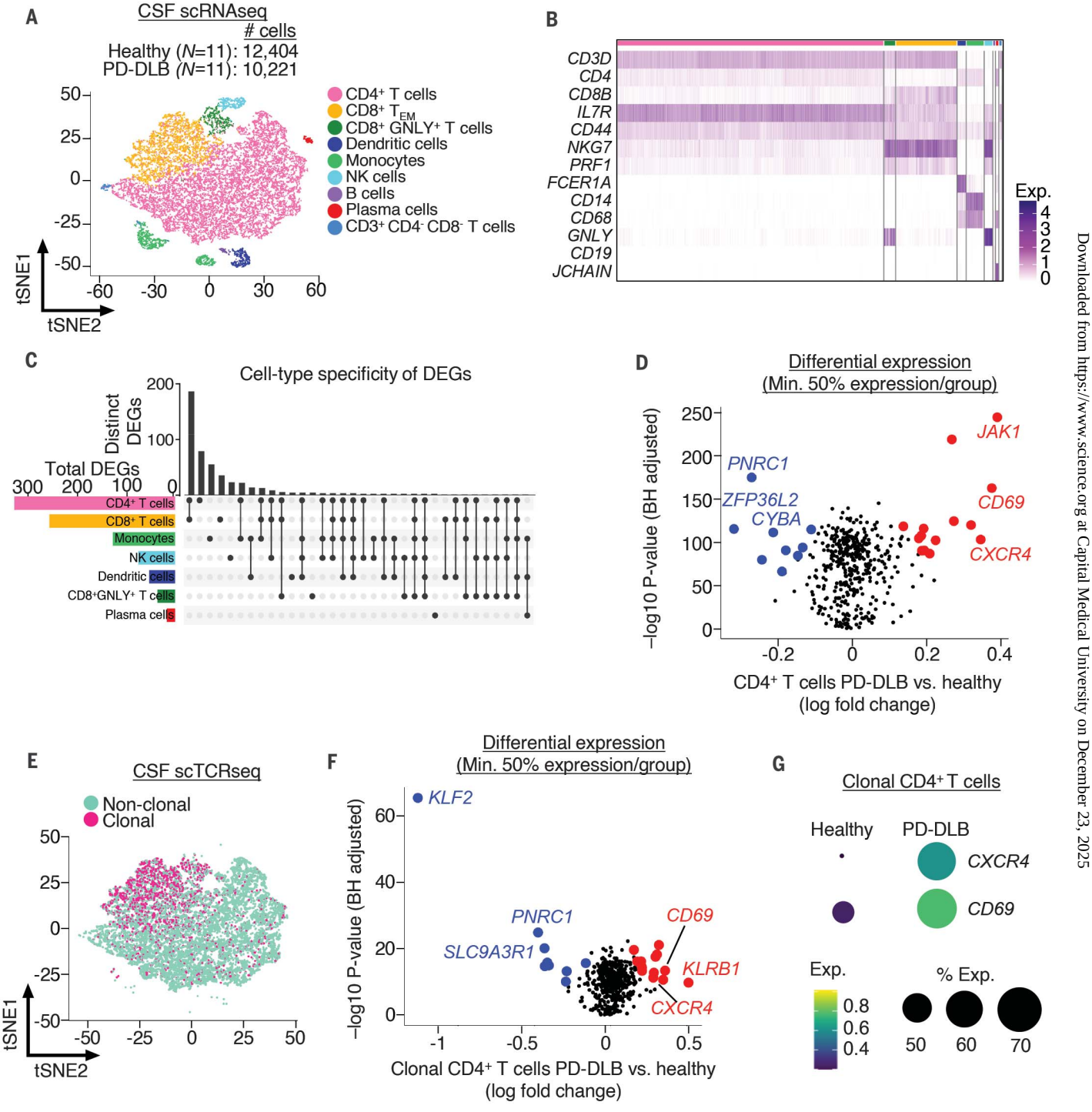

Fig. 2. Up-regulated *CXCR4* demarks $CD4^+$ T cells in PD-DLB. (**A**) scRNAseq of CSF cells shows clusters of various types of immune cells by tSNE. (**B**) Marker expression of CSF immune cells used to classify clusters. (**C**) UpSet plot showing cell-type–specific analysis of differentially expressed genes of PD-DLB versus healthy CSF immune cells indicating that the highest number of differentially expressed genes are in $CD4^+$ T cells. (**D**) Volcano plot showing differentially expressed genes of $CD4^+$ T cells from LBD versus healthy CSF. The increased expression of *CXCR4* in LBD is apparent. (**E**) scTCRseq of CSF immune cells showing clonal versus nonclonal T cells plotted by tSNE. (**F**) Volcano plot of differential expression analysis of clonal $CD4^+$ T cells showing increased expression of *CD69*, *KLRB1*, and *CXCR4* in PD-DLB versus healthy CSF. (**G**) Dot plot showing higher levels of *CXCR4* and *CD69* in PD-DLB versus healthy CSF clonal $CD4^+$ T cells.

Corrected 18 April 2024. See full text.

on PDD meninges, which revealed meningeal $CD3^+CXCR4^+$ cells (fig. S7A). We noted localization of the CXCR4 ligand, C-X-C motif chemokine ligand 12 (CXCL12) to $CD3^+CXCR4^+$ cells in the meninges (fig. S7A). In mice, CXCL12 is expressed by cerebrovascular endothelial cells and promotes recruitment of $CD4^+$ T cells (*19*). Within the PDD brain, CXCL12 localized to the cerebrovasculature (Fig. 3A), which we confirmed by costaining PDD brains with the vascular marker cluster of differentiation 31 (CD31; fig. S7B). $CD3^+$ T cells resided in the perivascular space adjacent to $CXCL12^+$ vessels (Fig. 3A and fig. S7C).

We next sought to determine whether levels of CSF CXCL12 were associated with cognitive impairment in PD. We measured CXCL12 in a cohort of age- and sex-matched healthy (n = 84) and PD (n = 79) subjects (fig. S8A). This revealed higher amounts of CSF CXCL12 in PD (Welch's t test, P = 0.036; Fig. 3B). We separated this PD cohort by clinical diagnoses as PD-NCI or PDD, which revealed lower cognitive scores in PDD subjects compared to healthy ($P = 3.12 \times 10^{-11}$) and PD-NCI ($P = 7.67 \times 10^{-10}$) subjects {one-way analysis of variance (ANOVA), [F (2,135) = 31.697, $P = 5.18 \times 10^{-12}$]; fig. S8B}. NEFL levels also distinguished PDD from healthy ($P = 1.00 \times 10^{-4}$) and PD-NCI ($P = 8.30 \times 10^{-3}$) subjects {one-way ANOVA, [F (2,117) = 9.161, P = 0.0002]; fig. S8C}. Age did not significantly affect CXCL12 levels in this cohort {analysis of covariance (ANCOVA) [F (2,150) = 2.867, P = 0.071]; fig. S8D}. We then correlated CXCL12 levels with neurodegenerative disease biomarkers, including ubiquitin carboxyl-terminal esterase L1, total tau, phosphorylated tau 181, amyloid-β, α-synuclein, and NEFL (fig. S8E). CXCL12 levels correlated most positively with NEFL in PDD [Spearman's rank correlation coefficient (r_s) = 0.40; P = 0.023), and these correlations were lesser in healthy (r_s = 0.12; P = 0.394) and PD-NCI ($_s$ = 0.17; P = 0.326) subjects {ANCOVA, [F (2,114) = 3.484, P = 0.031]; Fig. 3C}. Thus, dysregulated CXCR4-CXCL12 signaling is associated with neurodegeneration in LBD.

CXCR4 demarks $CD4^+$ T cells that are specific to the CSF

Because peripheral T cells have been shown to be dysregulated in PD (*4*, *5*, *14*), we compared $CD4^+$ T cells of the peripheral immune system and CSF. We performed scRNAseq on peripheral blood mononuclear cells (PBMCs) of the same subjects that we analyzed by CSF scRNAseq and focused our analysis on $CD4^+$ T cells (Fig. 4A). We uncovered $CD4^+$ T cell populations that were specific to the CSF (referred to as CSF unique; Fig. 4B). We also identified up-regulated *CXCR4*, *CD69*, and *TSC22 domain family member 3* (*TSC22D3*) as the primary genes defining CSF unique T cells (Fig. 4D). Quantification of individual subjects' CSF unique $CD4^+$ T cell *CXCR4* and *CD69* expression revealed higher levels in PD-DLB versus healthy CSF (Welch's t test, P = 0.0218 and P = 0.0217, respectively; Fig. 4E). Thus, *CXCR4* may regulate homing of $CD4^+$ T cells to the LBD brain.

α-synuclein stimulation drives T cell clonal expansion and activation

Our immunohistochemistry results indicated close proximity of T cells with α-synuclein in LBD brains. This led us to investigate whether α-synuclein could drive T cell clonal expansion and activation. Several peptides derived from α-synuclein act as antigenic epitopes and promote T cell responses in PD PBMCs (*4*, *5*). We incubated PBMCs from healthy (n = 32) and PD (n = 53) subjects with a pool of eight antigenic α-synuclein peptides and measured activation of $CD3^+$ T cells by flow cytometry using coexpression of HLA-DR and CD38 (fig. S9A). Unexpectedly, control PD patient T cells in the absence of stimulation exhibited higher percentages of $HLA\text{-}DR^+CD38^+$ T cells than healthy subjects (Welch's t test, P = 0.006; fig. S9, B and C), suggesting that higher baseline levels of peripheral T cell activation exists in PD patients in vivo. We also detected higher levels of T cell activation after stimulation with the α-synuclein peptide pool (Welch's t test, P = 0.002; fig. S10C). We confirmed increased activation of PD T cells after α-synuclein stimulation by measuring CD69 by flow cytometry (Welch's t test, P = 0.027; fig. S9D).

To identify patient-specific antigenic α-synuclein peptides, we selected two PD patients who exhibited appreciable increases in T cell activation by the α-synuclein peptide pool (fig. S9E). We then measured T cell activation in these subjects using individual α-synuclein peptides. This strategy revealed activation of T cells by the peptide DNEAYEMPSEEGYQD, which contains a phosphorylated serine residue at amino acid position 129 (Fig. 5, A and B). $HLA\text{-}DR^+CD38^+CD4^+$ T cells up-regulated CXCR4 in response to peptide stimulation (Fig. 5C). To determine transcriptional changes induced by this peptide, we sorted activated T cells from unstimulated and stimulated PBMCs (fig. S10A). We then performed scRNAseq on $HLA\text{-}DR^+CD38^+$ T cells to interpret transcriptomic alterations (data S4). Stimulated T cells had increased expression of *actin gamma*

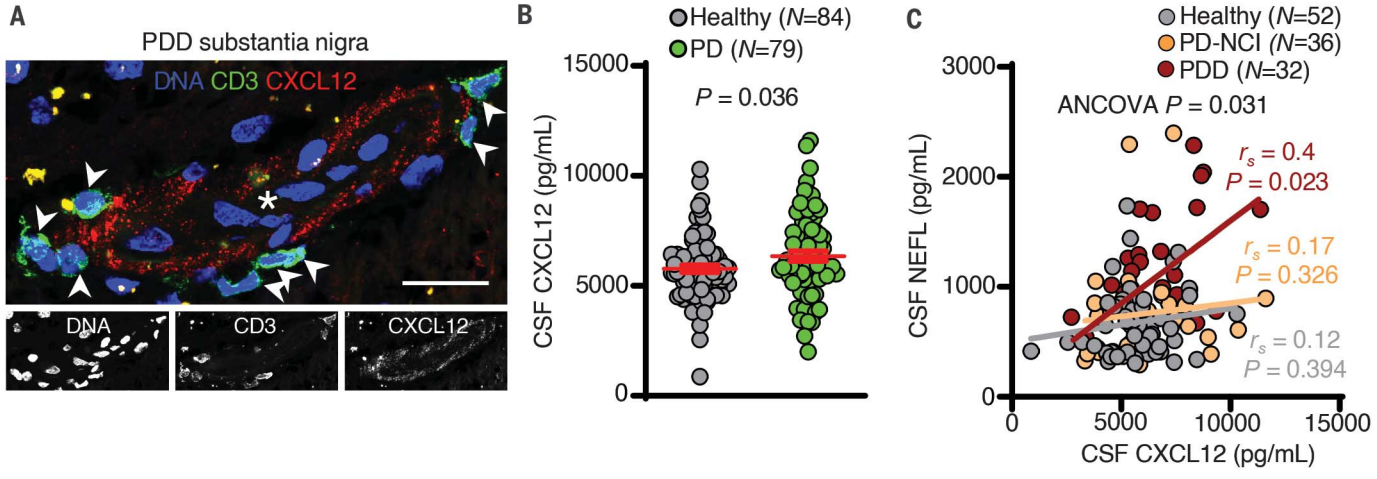

Fig. 3. CXCL12 is associated with neurodegeneration in LBD. (**A**) A PDD substantia nigra brain blood vessel showing localization of CXCL12 to the cerebral vasculature. Arrowheads indicate $CD3^+$ T cells in the perivascular space. Asterisk indicates blood vessel lumen. Scale bar, 50 μm. Similar results were observed in seven out of seven LBD brains. (**B**) Single-molecule array measurement of CXCL12 indicating higher levels in PD versus healthy CSF. Data are mean ± SEM. (**C**) Regression analysis correlating CSF CXCL12 and NEFL levels in healthy, PD-NCI, and PDD. There is a significant correlation of CXCL12 and NEFL in PDD but not PD-NCI or healthy CSF.

Corrected 18 April 2024. See full text.

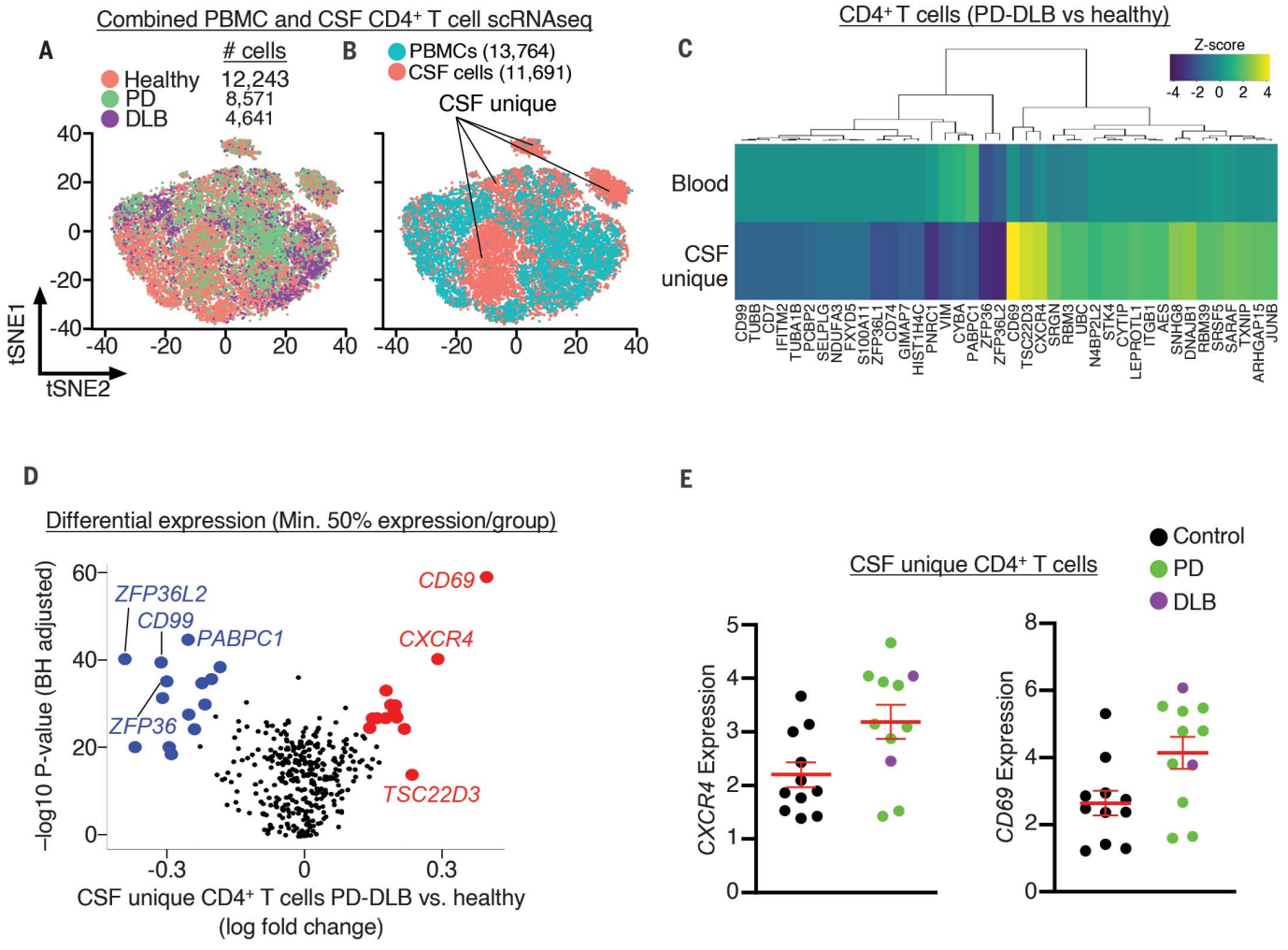

Fig. 4. CXCR4 demarks CD4$^+$ T cells that are specific to the CSF in LBD. (**A**) tSNE plot showing overlayed distribution of peripheral versus CSF CD4$^+$ T cells from healthy, PD, and DLB subjects. (**B**) tSNE plot showing clusters of CD4$^+$ T cells that are specific to the CSF. (**C**) Hierarchical clustering of standardized z-scores comparing PD-DLB to healthy CD4$^+$ T cells from PBMCs and CSF. The clustering of genes *CXCR4*, *CD69*, and *TSC22D3* demarks CSF unique CD4$^+$ T cells. (**D**) Volcano plot showing differential expression analysis comparing PD-DLB to healthy CSF unique CD4$^+$ T cells. (**E**) Quantification of individual subjects' *CXCR4* and *CD69* expression of PD-DLB versus healthy CSF unique CD4$^+$ T cells showing higher expression of each gene in PD-DLB. Data are mean ± SEM.

1 (*ACTG1*) and *actin beta* (*ACTB*) (Fig. 5D), which regulate cytoskeletal control of antigen-dependent T cell activation (*20*). We also noted increased expression of *marker of proliferation Ki-67* (*MKI67*), suggesting increased proliferation of stimulated T cells (Fig. 5D).

T_H17 cell involvement in the degeneration of neurons in LBD

Notably, we also detected higher expression of *interleukin 17A* (*IL17A*) in cells stimulated with α-synuclein (Fig. 5D). *IL17A* encodes the proinflammatory cytokine IL-17, which is secreted by T_H17 cells (*21*). To determine whether *IL17A*-expressing cells were clonally expanded, we performed scTCRseq on stimulated and unstimulated cells. This revealed clonal populations from stimulated cells of both patients (fig. S10B). We then plotted *IL17A* expression by tSNE and identified clonally expanded TCRs (clonotypes) from each subject (Fig. 5E). *IL17A*-expressing cells coexpressed *CD4*, and some clonotypes also expressed the T_H17-associated cytokine gene *interleukin 22* (*IL22*; fig. S10C). We confirmed the presence of CD4$^+$IL-17A$^+$ T cells in the PDD substantia nigra, which were adjacent to TH$^+$IL-17A$^+$ neurons (Fig. 5F). We also detected higher levels of IL-17A immunoreactivity in LBD brains (Welch's *t* test, $P = 0.007$; Fig. 5G). Public datasets revealed lack of *IL17A* RNA expression in the brain, yet the gene encoding the IL17A receptor, *IL17RA*, was highly expressed in the midbrain (fig. S11A), suggesting an external source of IL17A protein in neurons. Public histology data indicated an age-dependent accumulation of IL17A in neurons (fig. S11B). Finally, to confirm IL17A antibody specificity, we preincubated antibodies with recombinant IL-17A, which ablated IL-17A immunoreactivity (fig. S11C).

Discussion

In conclusion, these results implicate T_H17 cell involvement in the degeneration of neurons in LBD. Notably, CXCR4 regulates cell migration (*22*), and antagonism of CXCR4 modulates the pathogenicity of T_H17 cells (*23*). Thus, our investigation of intrathecal immunity uncovered the CXCR4-CXCL12 signaling axis as a potential therapeutic target for LBD. Several CXCR4 antagonists are currently approved for clinical use to treat a wide variety of diseases (*24*–*30*). Given the safety, bioavailability, and tolerability of CXCR4 antagonists (*26*), these drugs could be utilized to inhibit trafficking of pathological T_H17 cells into the LBD brain. Finally, we identified an antigenic α-synuclein epitope

Corrected 18 April 2024. See full text.

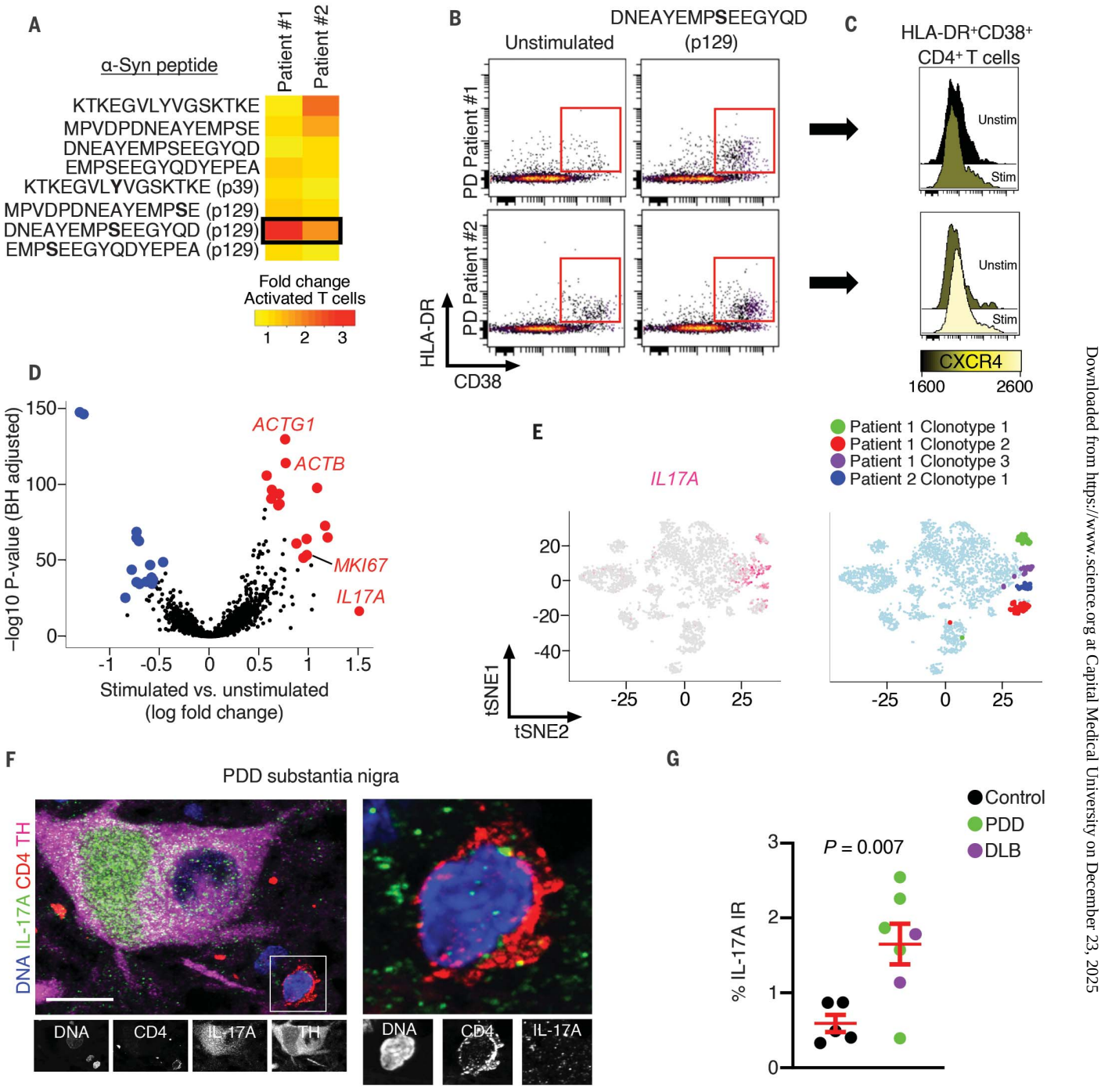

Fig. 5. Stimulation of LBD T cells with α-synuclein promotes *IL-17A* expression. (**A**) Heatmap showing fold change of T cell activation (percent HLA-DR$^+$CD38$^+$ CD3$^+$ T cells) between unstimulated and stimulated PBMCs. Cells were incubated with α-synuclein peptides known to be antigenic. Peptide DNEAYEMPSEEGYQD (p129) increased T cell activation in patients #1 and #2. (**B**) Flow cytometry plots of unstimulated and DNEAYEMPSEEGYQD (p129)–stimulated cells showing increased T cell activation (percent HLA-DR$^+$CD38$^+$ CD3$^+$ T cells) by the α-synuclein peptide. Abbreviations for the amino acid residues are as follows: A, Ala; C, Cys; D, Asp; E, Glu; F, Phe; G, Gly; H, His; I, Ile; K, Lys; L, Leu; M, Met; N, Asn; P, Pro; Q, Gln; R, Arg; S, Ser; T, Thr; V, Val; W, Trp; and Y, Tyr. (**C**) Histograms showing increased expression of CXCR4 in DNEAYEMPSEEGYQD (p129)–stimulated HLA-DR$^+$CD38$^+$CD4$^+$ T cells in both patients by flow cytometry. (**D**) Differential expression analysis of stimulated versus unstimulated HLA-DR$^+$CD38$^+$CD3$^+$ T cells shows increased expression of antigen-dependent T cell activation genes *ACTG1* and *ACTB*, the proliferative gene *MKI67*, and the proinflammatory cytokine *IL17A*. (**E**) tSNE plots indicating overlap of cells expressing *IL17A* and clonally expanded T cells (clonotypes) from both patients. (**F**) Confocal images of control (non-neurologic disease) and PDD postmortem brains showing CD4$^+$IL-17A$^+$ T cells adjacent to an IL-17A$^+$TH$^+$ neuron in the PDD substantia nigra. Scale bar, 10 μm. (**G**) Quantification of IL-17A immunoreactivity (IR) in the substantia nigra of control and LBD brains showing increased IL-17A in LBD. Similar results were observed in six out of seven LBD brains. Data are mean ± SEM.

that promoted expression of *IL17A*, a pro-inflammatory cytokine involved in autoimmune diseases (*21*). In animal models of neurodegenerative disease, T_H17 cells play a direct role in neuronal loss (*31*, *32*). Moreover, human T_H17 cells have been shown to promote blood-brain barrier disruption and central nervous system inflammation via IL-17A (*33*). Thus, our study provides a mechanism for T_H17 cell–mediated dopaminergic cell death through secretion of inflammatory IL-17A, thereby implicating autoimmunity in LBD (fig. S12).

REFERENCES AND NOTES

1. M. J. Armstrong, M. S. Okun, *JAMA* **323**, 548–560 (2020).
2. Z. Walker, K. L. Possin, B. F. Boeve, D. Aarsland, *Lancet* **386**, 1683–1697 (2015).
3. M. Iba *et al*., *J. Neuroinflammation* **17**, 214 (2020).
4. C. S. Lindestam Arlehamn *et al*., *Nat. Commun.* **11**, 1875 (2020).
5. D. Sulzer *et al*., *Nature* **546**, 656–661 (2017).
6. A. Sommer *et al*., *Cell Stem Cell* **23**, 123–131.e6 (2018).
7. G. T. Kannarkat, J. M. Boss, M. G. Tansey, *J. Parkinsons Dis.* **3**, 493–514 (2013).
8. J. A. Saunders *et al*., *J. Neuroimmune Pharmacol.* **7**, 927–938 (2012).
9. C. H. Stevens *et al*., *J. Neuroimmunol.* **252**, 95–99 (2012).
10. V. Brochard *et al*., *J. Clin. Invest.* **119**, 182–192 (2009).
11. C. Cebrián *et al*., *Nat. Commun.* **5**, 3633 (2014).
12. A. S. Harms *et al*., *J. Neurosci.* **33**, 9592–9600 (2013).
13. Z. Liu, Y. Huang, B. B. Cao, Y. H. Qiu, Y. P. Peng, *Mol. Neurobiol.* **54**, 7762–7776 (2017).
14. A. Singhania *et al*., *Sci. Rep.* **11**, 302 (2021).
15. D. Gate *et al*., *Nature* **577**, 399–404 (2020).
16. H. Oh *et al*., *Mol. Neurodegener.* **16**, 3 (2021).
17. L. Maggi *et al*., *Eur. J. Immunol.* **40**, 2174–2181 (2010).
18. K. L. Truong *et al*., *Nat. Commun.* **10**, 2263 (2019).
19. E. E. McCandless, Q. Wang, B. M. Woerner, J. M. Harper, R. S. Klein, *J. Immunol.* **177**, 8053–8064 (2006).
20. H. Colin-York *et al*., *Cell Rep.* **26**, 3369–3379.e5 (2019).
21. L. Steinman, *Nat. Med.* **13**, 139–145 (2007).
22. D. J. Campbell, C. H. Kim, E. C. Butcher, *Immunol. Rev.* **195**, 58–71 (2003).
23. D. Tischner *et al*., *JCI Insight* **2**, e95063 (2017).
24. Y. Iwasaki *et al*., *Cancer Sci.* **100**, 778–781 (2009).
25. T. Murakami *et al*., *Antimicrob. Agents Chemother.* **53**, 2940–2948 (2009).
26. N. D. Stone *et al*., *Antimicrob. Agents Chemother.* **51**, 2351–2358 (2007).
27. G. A. Donzella *et al*., *Nat. Med.* **4**, 72–77 (1998).
28. B. Nervi *et al*., *Blood* **113**, 6206–6214 (2009).
29. U. M. Domanska *et al*., *Neoplasia* **14**, 709–718 (2012).
30. H. Tamamura *et al*., *FEBS Lett.* **550**, 79–83 (2003).
31. A. Reboldi *et al*., *Nat. Immunol.* **10**, 514–523 (2009).
32. J. Zhang, K. F. Ke, Z. Liu, Y. H. Qiu, Y. P. Peng, *PLOS ONE* **8**, e75786 (2013).
33. H. Kebir *et al*., *Nat. Med.* **13**, 1173–1175 (2007).

ACKNOWLEDGMENTS

We thank the clinical staffs of the Stanford and University of California San Diego Alzheimer's Disease Research Centers for their assistance acquiring patient samples. **Funding:** This work was supported by a National Institute of Neurologic Disease and Stroke K99/R00 Pathway to Independence Award (NS112458-01A1) (D.G.); an Irene Diamond Fund/AFAR Postdoctoral Transition Award in Aging (D.G.); a National Institutes of Health National Institute on Aging (NIA) F32 Fellowship (AG055255-01A1) (D.G.); the FFG Momentia Project 867741 (L.A.); Austrian Science Fund (FWF) Project P 31362- B34 (L.A.); FFG Project 867741 PMU FFF E-20/32/169-UNG (L.A.); the Howard Hughes Medical Institute (M.M.D.); NIH U19 AG065156, R01 NS115114, P30 AG066515, and P50 NS062684 (K.L.P.); Michael J. Fox Foundation for Parkinson's Research Grants 020756, 16921, and 18411 (K.L.P.); the Lewy Body Dementia Association (K.L.P.); Alzheimer's Drug Discovery Foundation (K.L.P.); Sanofi US Services, Inc. (K.L.P.); the Cure Alzheimer's Fund (T.W.-C.); the NOMIS Foundation (T.W.-C.); NIA R01 AG045034 05 (T.W.-C.); and the NIA-funded Stanford Alzheimer's Disease Research Center P50AG047366 (V.W.H.).
Author contributions: D.G. designed experiments and prepared the manuscript. D.G. conducted confocal microscopy, flow cytometry, and scRNAseq and scTCRseq. E.T., O.L., A.Y., T.F., A.K., and H.O. assisted with sequencing analysis. T.N. performed ex vivo α-synuclein stimulation experiments. M.S. assisted with clinical data analysis. D.C. performed sample processing of CSF and blood cells. K.S., M.S.U., and L.A. performed histology and analysis of Thy1-αSyn mice. V.W.H., D.R.G., M.M.D., and K.L.P. provided patient samples and assisted with study design. D.G. and T.W.-C. wrote and edited the manuscript. All authors read and approved the final manuscript. **Competing interests:** K.L.P. has stock options and has received paid consulting fees from CuraSen Therapeutics, Inc. **Data and materials availability:** The scRNAseq datasets analyzed during the current study are available in the Gene Expression Omnibus repository under accession numbers GSE141578 and GSE161192. Some control samples (HC9-HC17) from GSE134578 (*15*) are the same as in GSE141578. The samples are included in both Gene Expression Omnibus datasets for convenience.

SUPPLEMENTARY MATERIALS

science.org/doi/10.1126/science.abf7266
Materials and Methods
Figs. S1 to S12
Table S1
References (*34*–*39*)
MDAR Reproducibility Checklist
Data S1 to S4

View/request a protocol for this paper from *Bio-protocol*.

16 November 2020; resubmitted 1 July 2021
Accepted 20 September 2021
Published online 14 October 2021
10.1126/science.abf7266